

# Influence of pH on the Formation of Benzyl Ester Bonds between Dehydrogenation Polymer and Cellulose

Wenhao Liu,<sup>a,b</sup> Xi Le,<sup>a,b</sup> Junjun Chen,<sup>a,b</sup> Junxian Xie,<sup>a,b</sup> Junjian An,<sup>a,b</sup> Guangyan Zhang,<sup>a,b</sup> Nianjie Feng,<sup>a,b</sup> Peng Wang,<sup>a,b</sup> \* and Yimin Xie<sup>a,b</sup>

Generation of lignin-carbohydrate complex (LCC) between dehydrogenation polymer (DHP) and pulp fibers may have an important impact on the properties of pulp. In this work, the benzyl ester-type LCC was formed between oxidized cellulose and DHP. The effect of pH on the addition reaction of oxidized cellulose to quinone methide in the synthesis of DHP-cellulose complex (DHPCC) was investigated. The structure of the product was characterized by Fourier Transform Infrared (FTIR), Carbon 13-Nuclear Magnetic Resonance (<sup>13</sup>C-NMR), and 2-Dimensional Heteronuclear Single Quantum Coherence Nuclear Magnetic Resonance (2D HSQC NMR) analyses. The results indicated that cellulose was indeed oxidized and carboxyl groups were introduced into cellulose by the oxidation process. The formed DHPCC was connected by benzyl ester linkage. In addition, the pH of the reaction system had an important role in the formation of the benzyl ester bonds. The acidic condition (pH = 4.0) was conducive to the addition reaction of quinone methide with carboxyl groups of cellulose. Overall, this study provides helpful guidance for the generation of LCC between DHP and paper pulp fibers.

DOI: 10.15376/biores.19.3.4238-4249

Keywords: Dehydrogenation polymer; Oxidized cellulose; Quinone methide; Benzyl ester bond

Contact information: a: Hubei Provincial Key Laboratory of Green Materials for Light Industry, Hubei University of Technology, 430068, Wuhan, China; b: School of Materials and Chemical Engineering, Hubei University of Technology, 430068, Wuhan, China; \*Corresponding author: ahwp1234@163.com

## INTRODUCTION

The presence of lignin in pulp fibers, such as unbleached kraft pulp, can lead to the formation of phenoxy radicals on the fiber surface through the catalytic action of lignin oxidases. The coupling of these phenoxy radicals enhances inter-fiber bonding, thereby improving the tensile strength of paper, particularly with regard to its wet strength. (Wong *et al.* 1999; Lund and Felby 2001; Liu *et al.* 2009). Due to the distance between phenoxy radicals generated from lignin on the fiber surface, the efficiency of radical coupling is low. Therefore, lignin peroxidase is utilized to catalyze the generation of dehydrogenation polymer (DHP) from phenolic compounds. The generated radicals on the DHP molecules facilitate their interaction with surface radicals present on fibers, enabling DHP to adhere to the fibers and thereby increasing the bonding strength between them (Yamaguchi *et al.* 1994; Chandra *et al.* 2002, 2004, 2005; Aracri *et al.* 2011). Although the enzyme-modified fiber can greatly improve the wet strength of paper, the dry strength is not significantly enhanced, which indicates that the bonding strength between fibers cannot be effectively improved by relying on the free radical coupling of fiber and DHP (Aracri *et al.* 2012). The

reason is attributed to the lignin content that can limit the formation of free radicals on the fiber surface.

In general, lignin and carbohydrate are connected in the form of lignin-carbohydrate complex (LCC), which gives wood excellent strength properties (Wang *et al.* 2016; Zhang *et al.* 2020). To investigate the structure and biosynthesis process of lignin, synthetic lignin DHP was prepared using lignin precursors under the action of lignin peroxidase (Terashima *et al.* 1995; Cathala and Monties 2001). In the authors' previous study, the authors simulated the synthetic environments of lignin and LCC in plants and used coniferin as the lignin precursor. The coniferin undergoes dehydrogenative polymerization catalyzed by laccase or peroxidase system to generate DHP, which has a similar structure to natural lignin. During the formation process, DHP underwent polymerization with pulp fibers, resulting in the establishment of robust bonds, including benzyl ether and benzyl ester linkages, which included linkages between DHP and plant fibers. The cooperative interaction significantly increased the wet strength properties of the resultant paper. Compared to the blank paper sample, the wet strength of the paper increased by 2.04 and 1.08 times, respectively (Wang *et al.* 2009a; Wang and Jian-Yun 2009). The above studies demonstrated that it was entirely possible for fibers to be connected to each other by DHP with LCC covalent bonds. However, there was no significant improvement in the dry strength of the paper, and the efficiency of LCC generation between DHP and fibers was not high. Therefore, to improve the dry and wet strengths of paper, it is necessary to produce LCC structures efficiently between DHP and fibers.

In plants, lignin precursors undergo dehydrogenation polymerization under the action of lignin oxidase, such as laccase, to produce phenolic oxygen radicals, which are continuously polymerized to produce lignin macromolecules. During the generation of lignin macromolecules, the quinone methide is generated through the polymerization of two free radicals. The carboxyl, hydroxyl groups, and water can undergo addition reactions with the quinone methide to generate benzyl ester-type and benzyl ether-type LCC linkages and  $\beta$ -O-4 lignin units, respectively (Fumiko *et al.* 1981; Watanabe and Koshijima 1988). The investigation into the native lignin structure elucidates the prevalence of the  $\beta$ -O-4 lignin unit, implying the predominance of addition reactions between water and quinone methide units in plants. In this context, a competitive relationship emerges, with carboxyl and hydroxyl groups vying for dominance within the reaction mechanism. Researchers used model compounds to demonstrate that acidic conditions favored the generation of benzyl ester-type LCC linkages (Tanaka *et al.* 1976, 1979; Brunow *et al.* 1989; Sipilä and Brunow 1991a,b,c). Wang *et al.* (2022) systematically investigated the effect of pH on the generation of benzyl ester-type LCC structures between DHP and glucuronic acid, and the results showed that acidic conditions were favorable for the addition reaction between the carboxyl group of glucuronic acid and the quinone methide in DHP. Therefore, this study hypothesizes that by increasing the amount of carboxyl groups on the surface of pulp fibers, an efficient addition reaction may occur between carboxyl groups and quinone methide in the DHP formation process, leading to the generation of a substantial number of benzyl ester linkages between DHP and fibers under appropriate reaction conditions.

Based on the above hypothesis, this study used the TEMPO/NaClO/NaBr (2,2,6,6-tetramethylpiperidinyloxy/sodium hypochlorite/sodium bromide) system to oxidize cellulose in paper pulp, resulting in the introduction of carboxyl groups on the cellulose macromolecule. The effect of pH on the formation of benzyl ester-type LCC between DHP

and paper pulp fibers was studied, providing guidance for the efficient generation of LCC between DHP and paper pulp fibers.

## EXPERIMENTAL

### Materials

Both coniferin-[side chain- $\alpha$ - $^{13}\text{C}$ ] and unlabeled coniferin were synthesized based on the previous report (Xie *et al.* 1994). A commercial bleached softwood kraft pulp was provided by a paper mill in Hubei province, China. Cellulase was obtained from Onozuka RS, Yakult Pharmaceutical Ind. Co. (Nishinomiya, Japan). Hemicellulase and  $\beta$ -glucosidase from almonds (specific activity: 6.3 units/mg) were supplied by Sigma-Aldrich (Shanghai, China). Laccase (E.C.1.10.3.2) was donated by Novozymes A/S (Tianjin, China). The (2,2,6,6-tetramethylpiperidin-1-yl) oxyl (TEMPO) used in this work was obtained from Macklin Biochemical Co., Ltd. (Shanghai, China). Sodium bromide and 12% sodium hypochlorite solution were purchased from Aladdin Industrial Corporation (Shanghai, China). Other chemicals were of laboratory grade obtained from Sinopharm Chemical Reagent Co., Ltd. (Shanghai, China) and used without further purification.

### Preparation of Cellulose from Pulp

The preparation of cellulose from pulp was performed based on reported research (Wei *et al.* 2018). Specifically, 20 g of dry pulp and 300 mL of 175 g/L NaOH solution was mixed in a 1000-mL beaker. The beaker was then mercerized in a water bath at 20 °C. After 90 min, 300 mL of distilled water was added, filtered, and washed with a Brinell's funnel until the washings were neutral, and then the filter cake was frozen to obtain cellulose.

### Oxidation of Cellulose

Approximately 10 g of dried cellulose was dispersed with 500 mL of distilled water. Then, TEMPO (50 mg) and NaBr (1.0 g) were added to the glass reaction vessel with an impeller stirrer to make a uniform mixing. When the sample was completely dispersed, the NaClO solution (4 mmol/g) was added to the reaction system and started timing the reaction. The system pH was kept at 10.5 by adding NaOH dropwise (0.5 mol/L). When the time reached 2 h, the reaction was adjusted to pH of 7.0 with HCl (0.5 mol/L) solution to terminate the reaction. The sample was then washed with distilled water and set aside.

### Preparation of DHP-Cellulose Complex (DHPCC)

The oxidized cellulose (1 g) was dispersed in 50 mL buffer solutions of various pH values (0.2 M sodium acetate/acetic acid buffer solution for pH=4 and 0.2 M sodium phosphate buffer for pH=7). A mixture of coniferin-[side chain- $\alpha$ - $^{13}\text{C}$ ] (0.3 g) and unlabeled coniferin (0.5 g) were completely dissolved with the newly prepared 0.2 mol/L buffer.

Approximately 100 mg  $\beta$ -glucosidase ( $\geq 6$  U/mg) and 715 IU laccase were added to the dispersed solution of oxidized cellulose under aseptic conditions and mixed well. The coniferin was added dropwise using a constant-flow pump (24 h, 2 mL/h), and the reaction mixture was kept at room temperature (30 °C) for 1 day. After 24 h, the dropwise addition was terminated, and the reaction was supplemented with 50 mg of  $\beta$ -glucosidase and 715 IU of laccase. The reaction was continued for 6 days, and the crude products were

obtained by centrifugal isolation. After that, the crude products were washed several times with distilled water to completely remove the residual enzyme as well as the initiator of the reaction and freeze-dried. Then, the  $^{13}\text{C}$ -labelled DHPCC was obtained (coded DHPCC- $[\alpha\text{-}^{13}\text{C}]$ ). The schematic diagram of the preparation process of DHPCC is shown in Fig. 1.

The coniferin (0.8 g) was taken and treated as described above to obtain unlabeled DHP-cellulose complex (coded DHPCC-control).

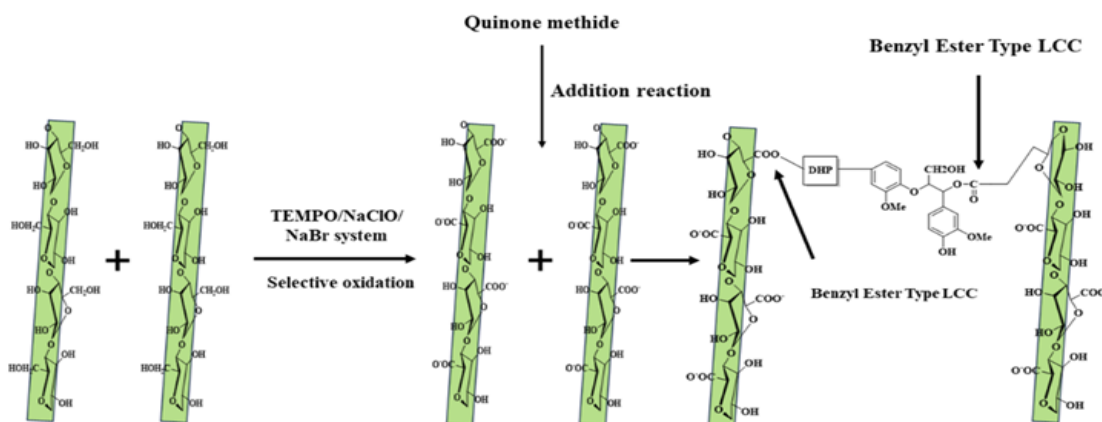


Fig. 1. The formation of the benzyl ester bond between plant fibers and DHP

### Ball Milling Treatment of DHPCC

The DHPCC was then taken to a planetary ball mill for mechanical treatment. The planetary ball mill ran for 30 min and stopped for 20 min with the cumulative working time of approximately 10 h. After the ball milling was completed, the DHPCC powder in the ball mill tank was removed for use.

### Enzymatic Degradation of DHPCC Treated with Ball Milling

The cellulase (0.5 g) and hemicellulase (0.5 g) were dissolved into a buffer solution (pH=4.5) containing 50 mL of acetic acid/sodium acetate solutions. The solution was filtered through a G3 sand-core funnel to remove water-insoluble material and then diluted to 150 mL. The 130 mL of enzyme solution was added to the dried DHPCC treated with ball milling, and then the sample was hydrolyzed in a shaking bath at 50 °C for 72 h. After the reaction, it was separated by centrifugation and washed with deionized water several times to obtain enzyme degraded DHPCC (coded as EDDHPCC).

### Alkali Treatment of DHPCC and EDDHPCC

The 100 mg sample was dissolved in 1.0 mol/L NaOH solution and stirred for 12 h at 25 °C under  $\text{N}_2$  atmosphere as a protective agent. After the reaction was completed, the pH was adjusted to acidic with dilute hydrochloric acid. The volume was set to 50 mL after precipitation. Subsequently, the liquid and precipitate were separated by centrifugation. The centrifuged liquid was frozen and then stored. The precipitate was washed with distilled water several times and freeze-dried for storage.

## Analytical Procedures

### FTIR characterization of DHPCC

Approximately 1 to 2 mg of DHPCC was mixed with 200 mg of anhydrous KBr, and then poured into a tablet die to form KBr pellet. The infrared analysis was performed by Thermo Fisher Nicolet (6700, Waltham, MA, USA).

### Cross Polarization/Magic Angle Spinning Carbon 13-Nuclear Magnetic Resonance (CP/MAS $^{13}\text{C}$ -NMR) spectra analysis of DHPCC

The solid-state CP/MAS  $^{13}\text{C}$ -NMR characterization was performed on an AV-III 400M spectrometer (Bruker Corp., Karlsruhe, Germany). The observing frequency used was 100.6 MHz and the acquisition time was 0.02 s. The proton  $90^\circ$  pulse time of 3.0 s with a 3.0 s pulse delay, and 3600 scans were accumulated.

### 2-Dimensional Heteronuclear Single Quantum Coherence Nuclear Magnetic Resonance 2D HSQC NMR analysis of EDDHPCC

The 2D-HSQC NMR was performed on a 500 MHz spectrometer (AVANCE III, Bruker, Germany). In detail, 50 mg samples were dissolved in 0.5 mL of DMSO- $d_6$  and then tested by nuclear magnetic resonance (NMR) for 8 h. The 5-mm wideband probe was used for 32 scans with a scanning delay of 1.0 s. Bruker standard pulse sequence: the sample data points of  $^1\text{H}$  dimension was 2048, and the sample data points of  $^{13}\text{C}$  dimension were 256. The spectral width used was 190 ppm in F1 ( $^{13}\text{C}$ ) and 11 ppm in F2 ( $^1\text{H}$ ).

## RESULTS AND DISCUSSION

### FTIR Analysis of DHPCC

Figure 2 shows the infrared spectra of DHPCC prepared at different pH values of 4.0 and 7.0 before and after alkali treatments.

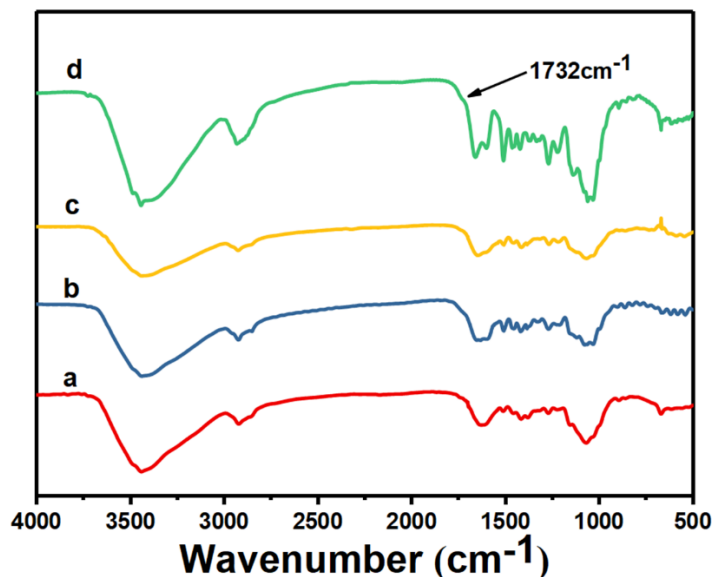


**Fig. 2.** Infrared spectra of DHPCC prepared at pH = 7.0 or 4.0 before and after alkali treatments: (a) after alkali treatment (pH = 7); (b) before alkali treatment (pH = 7); (c) after alkali treatment (pH = 4); (d) before alkali treatment (pH = 4)

It was observed that a shoulder peak of DHPCC that appeared at  $1732\text{ cm}^{-1}$  (pH = 4), due to the absorbance peaks of ester bonds and carboxyl groups. They disappeared in the infrared spectra after alkali treatment, which indicated that the peak was mainly due to the ester bond (Xie *et al.* 2000). In contrast, the DHPCC had no absorbance peak at  $1732\text{ cm}^{-1}$  (pH = 7.0) before and after alkali treatments. These results demonstrated that pH of 4.0 was conducive to the formation of benzyl ester bonds between carboxyl groups on cellulose and DHP. However, the intensity of the peaks suggested that the amount of ester bonding was not large.

### NMR Analysis of DHPCC

The CP/MAS  $^{13}\text{C}$ -NMR of DHPCC prepared under pH = 4.0 and pH = 7.0 before and after alkali treatments are depicted in Figs. 3 and 4, respectively. The chemical shifts (ppm) corresponding to the structural units contained in the DHPCC and their assignments were based on a previous study (Xie *et al.* 2000). The structural analysis in the sample was based on the intensity of the sugar absorbance peak (104 ppm). In this study, due to challenges in accurately quantifying the benzyl ester bond between cellulose and DHP,  $^{13}\text{C}$  tracer technology was employed specifically targeting the  $\alpha$ -C position of the DHP side chain.

The chemical shift of the benzyl ester bond formed between DHP and cellulose was observed around 73.0 ppm. Moreover, the susceptibility of the benzyl ester bond to alkaline degradation suggests a potential avenue for qualitative analysis utilizing  $^{13}\text{C}$  tracing coupled with alkali treatment. It can be seen from Figs. 3 and 4 that after oxidation using the TEMPO/NaClO/NaBr system, the cellulose had an absorbance peak at 173 ppm, which was attributed to the carboxyl absorbance peak on C<sub>6</sub> on the glucose structural unit. The results indicated that cellulose was oxidized, and carboxyl groups were introduced.

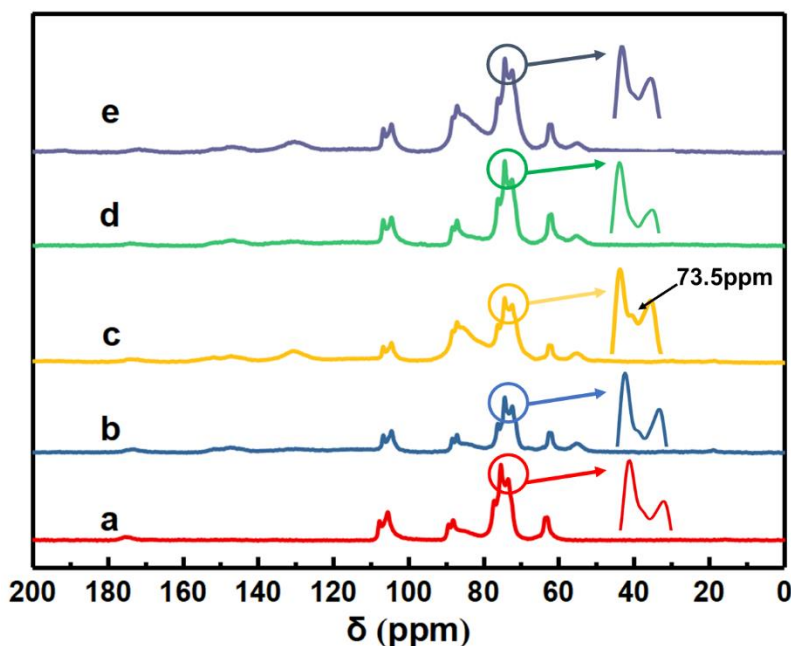


**Fig. 3** CP/MAS  $^{13}\text{C}$ -NMR spectra of DHPCC prepared under pH = 4.0 condition: (a) oxidized cellulose; (b) DHPCC-control; (c) EDDCC- $[\alpha\text{-}^{13}\text{C}]$ ; (d) EDDCC treated with alkali; (e) EDDCC- $[\alpha\text{-}^{13}\text{C}]$  treated with alkali

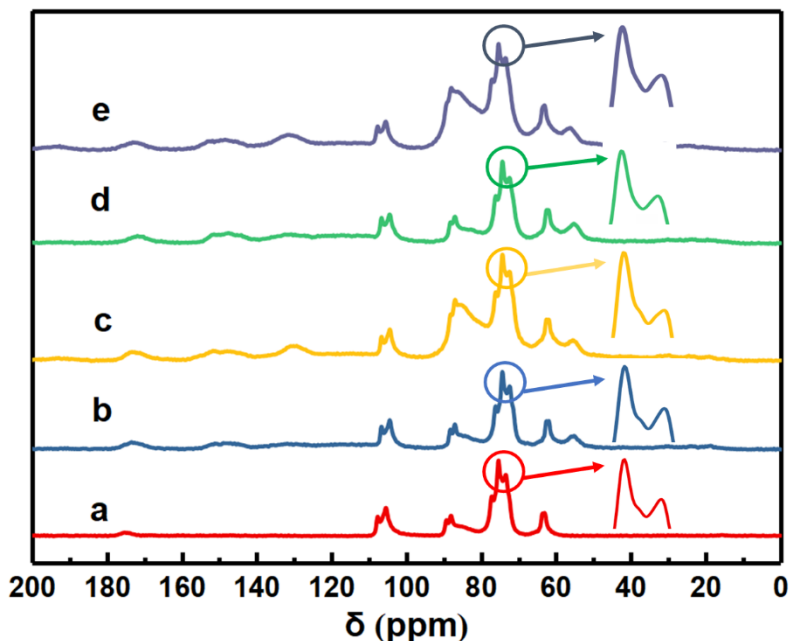


**Fig. 4.** CP/MAS  $^{13}\text{C}$ -NMR spectra of DHPCC prepared under pH = 7.0 condition: (a) oxidized cellulose; (b) DHPCC-control; (c) EDDCC- $[\alpha\text{-}^{13}\text{C}]$ ; (d) EDDCC treated with alkali; (e) EDDCC- $[\alpha\text{-}^{13}\text{C}]$  treated with alkali

Meanwhile, it can be seen from Fig. 3 that the DHPCC prepared under pH = 4.0 condition (after  $^{13}\text{C}$  labeled) had an absorbance peak at 73.5 ppm, and after alkali treatment, the peak disappeared. Therefore, it can be determined that this peak was related to the benzyl ester bond formed between the carboxyl group and DHP on the cellulose. As can be seen from Fig. 4 (after  $^{13}\text{C}$  labeled), there was no enhanced absorbance peak at 73.5 ppm. These results indicated that the carboxyl group on cellulose can easily form benzyl ester bonds with DHP under acidic conditions.

## 2D-HSQC NMR Spectrum Analysis of EDDHPCC

As shown in Fig. 5, although  $^{13}\text{C}$  tracer method can be used to detect the presence of benzyl ester bonds between DHP and cellulose, the intensity of the peaks was low. This was mainly because the chemical shift of benzyl ester bond overlapped with the chemical shift of cellulose, resulting in the peak enhancement of benzyl ester bond that was not obvious. To observe the absorbance peaks of the benzyl ester bond more clearly, the DHPCC was degraded using cellulase and hemicellulase to remove the cellulose that was not bound to DHP. The complex formed was then ball milled to make it dissolve in DMSO and enable 2D-HSQC NMR testing, which was displayed in Fig. 5.

The assignments and the main basic linkages in the structural unit are presented in Table 1 and Fig. 6 based on the reported literature (Brunow *et al.* 1989; Zhang *et al.* 2012; Tokunaga and Watanabe 2023), respectively. It can be observed that the side chain structure ( $\beta\text{-O-4}$ ,  $\beta\text{-5}$ , and  $\beta\text{-}\beta$ ) and aromatic structure ( $\text{G}_2$ ,  $\text{G}_5$ , and  $\text{G}_6$ ) of DHP were seen clearly on DHPCC prepared at pH = 4.0 and pH = 7.0. The results demonstrated that ball milling effectively enhanced the solubility of the complex while preserving its structural integrity.

**Table 1.** 2D-HSQC NMR spectra of EDDHPCC

| Label         | pH = 4                                    | pH = 4<br>(alkali)                        | pH = 7                                    | Assignments                                                            |
|---------------|-------------------------------------------|-------------------------------------------|-------------------------------------------|------------------------------------------------------------------------|
|               | $\delta_C/\delta_H$ (ppm)                 | $\delta_C/\delta_H$ (ppm)                 | $\delta_C/\delta_H$ (ppm)                 |                                                                        |
| C $_{\beta}$  | 52.68/3.45                                | 52.41/3.59                                | 52.90/3.45                                | C $_{\beta}$ -H $_{\beta}$ in phenylcoumaran (C)                       |
| B $_{\beta}$  | 53.48/3.03                                | 53.61/3.03                                | 53.45/3.04                                | C $_{\beta}$ -H $_{\beta}$ in $\beta$ - $\beta$ (resinol) (B)          |
| OCH $_3$      | 55.45/3.72                                | 55.38/3.74                                | 55.31/3.73                                | C-H in methoxyls                                                       |
| A $_{\gamma}$ | 60.02/3.22<br>60.37/3.78                  | 59.74/3.58<br>59.87/3.22                  | 59.74/3.23<br>60.52/3.42                  | C $_{\gamma}$ -H $_{\gamma}$ in $\beta$ -O-4 substructures (A)         |
| F $_{\gamma}$ | 61.53/4.07                                | 61.42/4.08                                | 61.34/4.08                                | C $_{\gamma}$ -H $_{\gamma}$ in cinnamyl alcohol end-groups (F)        |
| C $_{\gamma}$ | 62.51/3.57                                | 62.52/3.69                                | 62.50/3.70                                | C $_{\gamma}$ -H $_{\gamma}$ in phenylcoumaran (C)                     |
| B $_{\gamma}$ | 70.64/3.62<br>70.75/4.12                  | 70.67/3.74<br>70.69/4.13                  | 70.33/3.55<br>70.59/3.73<br>70.75/4.13    | C $_{\gamma}$ -H $_{\gamma}$ in $\beta$ - $\beta$ resinol (B)          |
| A $_{\alpha}$ | 71.09/4.71                                | 71.03/4.74                                | 70.94/4.72                                | C $_{\alpha}$ -H $_{\alpha}$ in $\beta$ -O-4 unit (A)                  |
| BE            | 73.71/5.88                                | ND                                        | ND                                        | Benzyl ester bond structure                                            |
| A $_{\beta}$  | 83.70/4.28                                | 83.60/4.29                                | 83.62/4.28<br>83.21/4.47                  | C $_{\beta}$ -H $_{\beta}$ in $\beta$ -O-4 substructures (A)           |
| A' $_{\beta}$ | 80.96/4.55                                | ND                                        | ND                                        | C $_{\beta}$ -H $_{\beta}$ in $\beta$ -O-4 linked to G (A)             |
| B $_{\alpha}$ | 84.90/4.61                                | 84.80/4.62                                | 84.67/4.62                                | C $_{\alpha}$ -H $_{\alpha}$ in $\beta$ - $\beta$ resinol (B)          |
| C $_{\alpha}$ | 86.92/5.45<br>87.76/5.58                  | 86.61/5.47<br>87.95/5.63                  | 86.67/5.45<br>87.37/5.58                  | C $_{\alpha}$ -H $_{\alpha}$ in phenylcoumaran (C)                     |
| G $_2$        | 110.44/6.91<br>111.21/7.32<br>112.34/7.20 | 110.94/6.96<br>109.50/7.38<br>112.31/7.42 | 110.14/6.91<br>111.04/7.34                | C $_2$ -H $_2$ in guaiacyl units (G)                                   |
| G $_5$        | 114.58/6.66<br>114.61/6.73<br>115.25/6.96 | 114.49/6.69<br>114.88/6.95                | 114.48/6.63<br>114.85/6.97                | C $_5$ -H $_5$ in guaiacyl units (G)                                   |
| G $_6$        | 118.61/6.75<br>118.63/6.83<br>120.42/6.74 | 118.50/6.84                               | 118.20/6.77<br>118.42/6.76<br>118.00/6.97 | C $_6$ -H $_6$ in guaiacyl units (G)                                   |
| G' $_6$       | 118.66/7.30                               | 119.95/7.52                               | 118.48/7.32                               | $\alpha$ C $_6$ -H $_6$ in G-type structural units with oxidized sites |
| E $_{\beta}$  | 126.14/6.75                               | ND                                        | 125.64/6.76                               | C $_{\beta}$ -H $_{\beta}$ in cinnamyl aldehyde end-groups (E)         |
| Glu $_1$      | 102.63/4.31                               | 102.52/4.33                               | 102.42/4.33                               | C $_1$ /H $_1$ in $\alpha$ -D-glucopyranoside                          |

Comparing Fig. 5a with Fig. 5b, two small, but noteworthy differences in the spectra are evident. In Fig. 5a, there was an absorbance peak at  $\delta C/\delta H$  73.71/5.88 ppm, while there was no such peak found in Fig. 5b. Meanwhile, the absorbance peak in Fig. 5a was much stronger in intensity than that in Fig. 5b at  $\delta C/\delta H$  102.52-102.63/4.31-4.33 ppm, which corresponded to C $_1$ /H $_1$  in  $\alpha$ -D-glucopyranoside from DHPCC. Because the benzyl ester bond was easily broken by alkali when the complex was subjected to alkali treatment. The 2D-HSQC NMR spectra of EDDHPCC prepared at pH = 4.0 after alkali treatment is depicted in Fig. 5c. Comparing Fig. 5a with Fig. 5c, the impact of alkali treatment on the complex was evident. The chemical shift at  $\delta C/\delta H$  73.71/5.88 ppm was notably absent after the treatment, indicating that the absorbance peak at  $\delta C/\delta H$  73.71/5.88 ppm was due to a benzyl ester bond.



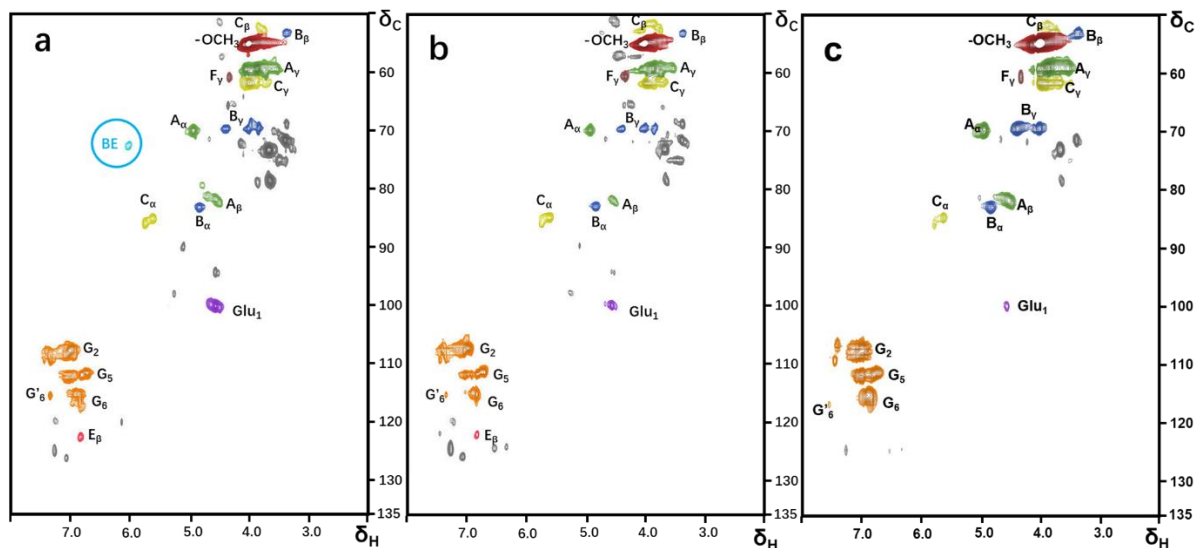


**Fig. 5.** (a) 2D-HSQC NMR spectra of EDDHPCC prepared at pH = 4.0; (b) 2D-HSQC NMR spectra of EDDHPCC prepared at pH = 7.0; and (c) 2D-HSQC NMR spectra of EDDHPCC prepared at pH = 4.0 after alkali treatment

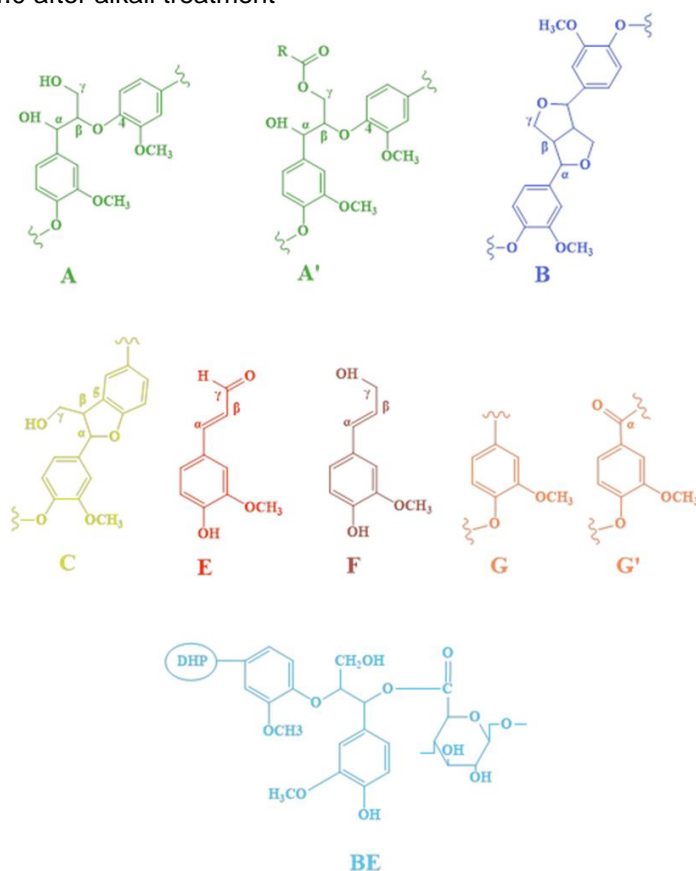


**Fig. 6.** The main basic linkages in the structural unit of the side chain region and aromatic ring region in the 2D-spectrum of the DHPCC: A:  $\beta$ -O-4 Ether bond structure ( $\gamma$ -hydroxyl); A':  $\beta$ -O-4 Ether bond structure ( $\gamma$ -acetyl group); B: Resinol structure, composed of  $\beta$ - $\beta$  and  $\alpha$ -O- $\gamma$ '; C: Phenylcoumarine structure, composed of  $\beta$ -5 and  $\alpha$ -O-4 connections; E: Coniferaldehyde unit; F: Coniferol unit; G: Guaiacyl-based structure; G': Oxidized guaiacyl-based structure; BE: Benzyl ester bond structure

Meanwhile, Fig. 5c showed that the intensity of absorbance peak decreased remarkably at  $\delta C/\delta H$  102.52-102.63/4.31-4.33 ppm, which indicated the reduction of carbohydrates in DHPCC. This was due to the breaking of the benzyl ester bond, which caused the cellulose to free itself from the complex. Combined with the disappearance of the absorbance peak at  $\delta C/\delta H$  73.71/5.88 ppm, it could be concluded that the benzyl ester bond was broken during the alkali treatment of the EDDHPCC. Correspondingly, the DHP-cellulose connection was broken, the cellulose was separated from the DHP and removed during subsequent DHP acid precipitation, centrifugation, and washing process. The 2D-HSQC NMR results showed that the carboxyl group on cellulose was easy to form benzyl ester bonds with DHP under acidic conditions.

## CONCLUSIONS

The pH value of the reaction system was found to have a significant impact on the formation of benzyl ester bonds between dehydrogenation polymer (DHP) and fibers of paper pulp. Acidic conditions (pH=4.0) favored the addition reaction of carboxyl groups on the surface of pulp fiber introduced by TEMPO/NaClO/NaBr oxidation of cellulose in paper pulp with quinone methide intermediates generated during dehydrogenative polymerization of coniferin, which can efficiently generate benzyl ester bonds between DHP and fibers of paper pulp. This conclusion provides a new method for improving paper strength through benzyl ester bonds between pulp fibers.

## ACKNOWLEDGMENTS

This study was financially supported by the National Natural Science Foundation of China (No. 32071722 and No. 31300494).

## REFERENCES CITED

- Aracri, E., Roncero, M. B., and Vidal, T. (2011). "Studying the effects of laccase-catalyzed grafting of ferulic acid on sisal pulp fibers," *Bioresource Technology* 102(16), 7555-7560. DOI: 10.1016/j.biortech.2011.05.046
- Aracri, E., Valls, C., and Vidal, T. (2012). "Paper strength improvement by oxidative modification of sisal cellulose fibers with laccase-TEMPO system: Influence of the process variables," *Carbohydrate Polymers* 88(3), 830-837. DOI: 10.1016/j.carbpol.2012.01.011
- Brunow, G., Sipilä, J., and Mäkelä, T. (1989). "On the mechanism of formation of non-cyclic benzyl ethers during lignin biosynthesis. Part 1. The reactivity of  $\beta$ -O-4 quinone methides with phenols and alcohols," *Holzforschung* 43(1), 55-59. DOI: 10.1515/hfsg.1989.43.1.55
- Cathala, B., and Monties, B. (2001). "Influence of pectins on the solubility and the molar mass distribution of dehydrogenative polymers (DHPs, lignin model compounds)," *International Journal of Biological Macromolecules* 29, 45-51. DOI: 10.1016/S0141-8130(01)00145-3

- Chandra, R. P., and Ragauskas, A. J. (2002). "Evaluating laccase-facilitated coupling of phenolic acids to high-yield kraft pulps," *Enzyme and Microbial Technology* 30(7), 855-861. DOI: 10.1016/S0141-0229(02)00020-0
- Chandra, R. P., Lehtonen, L. K., and Ragauskas, A. J. (2004). "Modification of high lignin content kraft pulps with laccase to improve paper strength properties. 1. Laccase treatment in the presence of gallic acid," *Biotechnology Progress* 20(1), 255-261. DOI: 10.1021/bp0300366
- Chandra, R. P., Felby, C., and Ragauskas, A. J. (2005). "Improving laccase-facilitated grafting of 4-hydroxybenzoic acid to high-kappa kraft pulps," *Journal of Wood Chemistry and Technology* 24(1), 69-81. DOI: 10.1081/WCT-120035945
- Fumiko, Y., Tanaka, R., and Koshijima, T. (1981). "Lignin carbohydrate complex. Pt. IV. Lignin as side chain of the carbohydrate in Björkman LCC," *Holzforschung* 35(4), 177-181. DOI: 10.1515/hfsg.1981.35.4.177
- Liu, N., Shi, S., Gao, Y., and Qin, M. (2009). "Fiber modification of kraft pulp with laccase in presence of methyl syringate," *Enzyme and Microbial Technology* 44(2), 89-95. DOI: 10.1016/j.enzmictec.2008.10.014
- Lund, M., and Felby, C. (2001). "Wet strength improvement of unbleached kraft pulp through laccase catalyzed oxidation," *Enzyme and Microbial Technology* 28(9-10), 760-765. DOI: 10.1016/S0141-0229(01)00339-8
- Sipilä, J., and Brunow, G. (1991a). "On the mechanism of formation of non-cyclic benzyl ethers during lignin biosynthesis. Part 3. The reactivity of a  $\beta$ -O-4-type quinone methide with methyl- $\alpha$ -d-glucopyranoside in competition with vanillyl alcohol. The formation and the stability of benzyl ethers between lignin and carbohydrates," *Holzforschung* 45(S1), 3-7. DOI: 10.1515/hfsg.1991.45.s1.3
- Sipilä, J., and Brunow, G. (1991b). "On the mechanism of formation of non-cyclic benzyl ethers during lignin biosynthesis. Part 2. The effect of pH on the reaction between a  $\beta$ -O-4-type quinone methide and vanillyl alcohol in water-dioxane solutions. The stability of non-cyclic benzyl aryl ethers during lignin biosynthesis," *Holzforschung* 45(4), 275-278. DOI: 10.1515/hfsg.1991.45.4.275
- Sipilä, J., and Brunow, G. (1991c). "On the mechanism of formation of non-cyclic benzyl ethers during lignin biosynthesis. Part 4. The reactions of a  $\beta$ -O-4-type quinone methide with carboxylic acids in the presence of phenols. The formation and stability of benzyl esters between lignin and carbohydrates," *Holzforschung* 45(S1), 9-14. DOI: 10.1515/hfsg.1991.45.s1.9
- Tanaka, K., Nakatsubo, F., and Higuchi, T. (1976). "Reactions of guaiacylglycerol-beta-guaiacyl ether with several sugars, 1: Reaction of quinonemethide with D-glucuronic acid," *Journal of the Japan Wood Research Society* 22(1), 589-590.
- Tanaka, K., Nakatsubo, F., and Higuchi, T. (1979). "Reactions of guaiacylglycerol-beta-guaiacyl ether with several sugars, 2: Reactions of quinonemethide with pyranohexoses," *Journal of the Japan Wood Research Society* 25(1), 653-659.
- Terashima, N., Atalla, R., Ralph, S., Landucci, L. L., Lapierre, C., and Monties, B. (1995). "New preparations of lignin polymer models under conditions that approximate cell wall lignification. I. Synthesis of novel lignin polymer models and their structural characterization by  $^{13}\text{C}$  NMR," *Holzforschung* 49(6), 521-527. DOI: 10.1515/hfsg.1995.49.6.521
- Tokunaga, Y., and Watanabe, T. (2023). "An investigation of the factors controlling the chemical structures of lignin dehydrogenation polymers," *Holzforschung* 77(1), 51-62. DOI: 10.1515/hf-2022-0129

- Wang, P. (2009a). "Study on crosslinking of unbleached softwood KP catalyzed by laccase (I)-Mechanism of reaction of coniferin with unbleached KP," *Paper Science and Technology* 28(03), 1-6.
- Wang, P., and Jian-Yun, F. (2009). "Study on crosslinking of unbleached kraft pulp catalyzed by peroxidase," *Transactions of China Pulp and Paper* 24(03), 33-36.
- Wang, P., Ye, Z., Wu, C., and Xie, Y. (2016). "Rebuilding of compound middle lamella of plant fibers and enhancement of paper strength," *Science and Technology Review* 34(19), 71-75. DOI: 10.5555/20163391799
- Wang, X., Le, X., Peng, W., Ye, P., An, J., Zhang, G., Wang, P., and Xie, Y. (2022). "Effect of pH on the formation of benzyl ester bonds between glucuronic acid and dehydrogenation polymer," *BioResources* 17(1), 52-63. DOI: 10.15376/biores.17.1.52-63
- Watanabe, T., and Koshijima, T. (1988). "Evidence for an ester linkage between lignin and glucuronic acid in lignin-carbohydrate complexes by DDQ-oxidation," *Agricultural and Biological Chemistry* 52(11), 2953-2955. DOI: 10.1080/00021369.1988.10869116
- Wei, Y., Huang, Y., Yu, Y., Gao, R., and Yu, W. (2018). "The surface chemical constituent analysis of poplar fibrosis veneers during heat treatment," *Journal of Wood Science* 64, 485-500. DOI: 10.1007/s10086-018-1732-x
- Wong, K. K., Anderson, K. B., and Kibblewhite, R. P. (1999). "Effects of the laccase-mediator system on the handsheet properties of two high kappa kraft pulps," *Enzyme and Microbial Technology* 25(1-2), 125-131. DOI: 10.1016/s0141-0229(99)00022-8
- Xie, Y., Robert, D., and Terashima, N. (1994). "Selective carbon 13 enrichment of side chain carbons of ginkgo lignin traced by carbon 13 nuclear magnetic resonance," *Plant Physiology and Biochemistry* 32, 243-249.
- Xie, Y., Yasuda, S., Wu, H., and Liu, H. (2000). "Analysis of the structure of lignin-carbohydrate complexes by the specific<sup>13</sup>C tracer method," *Journal of Wood Science* 46, 130-136. DOI: 10.1007/BF00777359
- Yamaguchi, H., Maeda, Y., and Sakata, I. (1994). "Bonding among woody fibers by use of enzymatic phenol dehydrogenative polymerization: Mechanism of generation of bonding strength," *Journal of the Japan Wood Research Society (Japan)* 40(2), 185-190. DOI: 10.1080/02773819408003114
- Zhang, F., Lan, X., Peng, H., Hu, X., and Zhao, Q. (2020). "A 'Trojan Horse' camouflage strategy for high-performance cellulose paper and separators," *Advanced Functional Materials* 30(32), article ID 2002169. DOI:10.1002/adfm.202002169
- Zhang, H., Li, W.-J., Nie, S.-P., Chen, Y., Wang, Y.-X., and Xie, M.-Y. (2012). "Structural characterisation of a novel bioactive polysaccharide from *Ganoderma atrum*," *Carbohydrate Polymers* 88(3), 1047-1054. DOI: 10.1016/j.carbpol.2012.01.061

Article submitted: March 22, 2024; Peer review completed: April 13, 2024; Revised version received and accepted: April 25, 2024; Published: May 9, 2024.  
DOI: 10.15376/biores.19.3.4238-4249